FUNDAMENTAL PROBLEMS IN STATISTICAL MECHANICS VI
E.G.D. Cohen, Editor

PHASE SEPARATION AND PATTERN FORMATION

J.S. LANGER

Institute for Theoretical Physics, University of California,
Santa Barbara, California 93106, U.S.A.

Lecture notes by

C.W.J. BEENAKKER

Instituut-Lorentz, Rijksuniversiteit te Leiden,
Nieuwsteeg 18, 2311 SB Leiden, The Netherlands

1. INTRODUCTION

In these lectures we shall deal with the theoretical description of the dynamics of a large class of first order phase transitions[1]. The basic physics of this subject is long known, going back at least to the days of van der Waals. Nevertheless, the theory is still very far from being complete, as we shall see. One of the most exciting areas of research in this field is the study of spontaneous pattern formation in phase-separating systems. Can we understand why, under some circumstances, water freezes in the form of a snow flake? Or, more generally, how are definite patterns selected in a structureless environment?

To be specific, we shall in the main part of these lectures talk about the precipitation of one of the components of a binary liquid mixture or alloy. Much of the theoretical formalism can, however, be applied straightforwardly to liquid-vapour and liquid-solid transitions in a pure substance. (We shall do so for the latter transition when we come to pattern formation.) Also, we shall restrict our attention to processes which are thermally activated; by this we mean that the transition is assumed to take place via the nucleation and growth of some characteristic disturbance of the homogeneous system, which is itself in a *metastable* state. Condensation of supercooled vapour, for example, is initiated by the formation of a sufficiently large droplet of liquid. Similarly, the phase separation in an alloy is nucleated by a critically large "grain" of precipitate. In particular, we shall not talk about the situation that a homogeneous system is driven into an *unstable* state (in which case the phase separation takes place via a process called *spinodal decomposition*).

The scheme of these lectures is as follows. In section 2 we discuss the basic physics of the theory of phase separation. Nucleation of droplets (or grains) will be considered only briefly. The subsequent droplet growth is examined in some detail in section 3. Section 4 is concerned with the onset of the shape instability of a growing spherical droplet and the emergence of structure in a particular destabilized system, viz. an isolated *dendritic* - that is, treelike - crystal growing from its undercooled melt. In this connection we shall also discuss a very promising recent model of pattern formation in solidification.

2. CONTINUUM THEORY OF PHASE SEPARATION

The phenomenological description of a first-order phase transition, initiated by van der Waals[2] [3] and reformulated and extended by Cahn and

Hilliard[4] and Fisk and Widom[5], postulates a free energy F of the form

$$F\{c\} = \int d\vec{r}\,[f(c(\vec{r})) + \frac{1}{2} K(\vec{\nabla}c(\vec{r}))^2], \tag{2.1}$$

which is a *functional* of the field $c(\vec{r})$. In the present context, $c(\vec{r})$ can be taken as the concentration at point $\vec{r}$ of one of the components of a binary fluid mixture or alloy. The integrand in the above expression consists of the free-energy density f(c) of a uniform state plus a first correction for deviations from uniformity, given by the square gradient of the concentration - with a coefficient K which, for simplicity, we shall assume independent of the concentration.

It is essential to note that the functional $F\{c\}$ has meaning only in the context of a coarse-graining or cellular description[6]. That is to say, the function $c(\vec{r})$ is assumed to be the average concentration in some small "cell" around the position $\vec{r}$ and is allowed to vary only slowly from cell to cell. A suitable size of the coarse-graining cells would be the correlation length of density fluctuations[7], so that on one hand each cell contains a large number of molecules, while on the other hand phase separation does not occur within single cells. In this description the function f(c) represents the free-energy density of a system which is constrained to have (with respect to the coarse-graining scale) a *uniform* concentration c. Below the critical temperature, f(c) will be a *non-convex* function, as sketched in fig. 1, different from the *convex* equilibrium free energy (which one could obtain by taking the size of the coarse-graining cells to be comparable to the size of the system). Because of this coarse-graining, f(c) is not a directly measurable quantity - what one might consider to be an unsatisfactory aspect of the van der Waals theory, as remarked by van Leeuwen in this school.

We turn now to the equations of motion. We start with the continuity equation for the conserved field $c(\vec{r})$

$$\partial c(\vec{r})/\partial t = - \vec{\nabla}\cdot\vec{j}(\vec{r}), \tag{2.2}$$

supplemented by a relation between the flux $\vec{j}(\vec{r})$ and the thermodynamic "force" $\vec{\nabla}\mu(\vec{r})$, which is the gradient of the local chemical potential $\mu(\vec{r})$. This quantity is obtained by taking the functional derivative of the free energy functional (2.1), $\mu(\vec{r}) = \delta F\{c\}/\delta c(\vec{r})$. We assume a linear relation between flux and force,

$$\vec{j}(\vec{r}) = - M(c)\vec{\nabla}\mu(\vec{r}), \tag{2.3}$$

with a mobility M which may itself be a function of the concentration. Eqs. (2.1)-(2.3) yield the nonlinear equation of motion

$$\frac{\partial c}{\partial t} = \vec{\nabla}\cdot M(c)\vec{\nabla}(\frac{df}{dc} - K\nabla^2 c), \tag{2.4}$$

studied extensively by Cahn, Hilliard and coworkers[8,9]. If we linearize this equation around the uniform solution $c(\vec{r}) \equiv c_0$ and look at spatial variations of c which are so slow that the square gradient term may be neglected (that is to say, c nearly constant over distances of order $\xi \equiv \sqrt{(K/f''(c_0))}$), we obtain a diffusion equation

$$\frac{\partial c}{\partial t} = D\nabla^2 c, \tag{2.5}$$

with a diffusion coefficient $D(c_0) = M(c_0)f''(c_0)$.

It is important to keep in mind that this thermodynamic description of phase separation can not be used to describe the kinetics of thermally activated processes, as nucleation, for which a free-energy barrier must be overcome. (To see this, just note that eqs. (2.2) and (2.3) imply that the free energy F decreases monotonically in time,

$$\frac{dF}{dt} = \int d\vec{r}\, \frac{\delta F}{\delta c}\frac{\partial c}{\partial t} = \int d\vec{r}\, \mu\vec{\nabla}\cdot M\vec{\nabla}\mu = -\int d\vec{r}\, M(\vec{\nabla}\mu)^2 \leq 0. \quad)$$

One way to deal with such a process is to add a stochastic "Langevin" force to the r.h.s. of eq. (2.4), which accounts for the effect of thermal fluctuations in the concentration. Alternatively[10], one can start from a Fokker-Planck type equation for the probability distribution functional defined on the space of functions $c(\vec{r})$. Here we shall not, however, discuss the nucleation theory that may be derived from such a model[11 12 13].

We now proceed to examine *stationary states*, characterized by a uniform chemical potential. The case $c(\vec{r}) \equiv c_0$ = constant is a trivial example of such a state. More interestingly, consider the case of two coexistent phases with a planar interface. We wish to calculate the density profile c(x), where the distance x is measured perpendicular to the interface. The bulk densities c_α and c_β of the coexistent phases α and β are obtained via the common-tangent construction in the plot of f(c) shown in fig. 1, from which one also finds the equilibrium chemical potential at coexistence μ_c (which is the slope of the tangent). Substituting expression (2.1) into the condition for a uniform chemical potential $\delta F/\delta c \equiv \mu_c$, one finds for the density profile the equation

$$\frac{df}{dc} - K\frac{d^2c}{dx^2} = \mu_c. \tag{2.6}$$

The solution of this equation has a form as in fig. 2; the density changes by $\delta c \equiv c_\beta - c_\alpha$ over a distance of order ξ, which in general is a microscopic length of a few angstroms.

If the interface between the coexistent phases is curved, the chemical potential of the stationary state necessarily differs from μ_c, say $\mu \equiv \mu_c + \delta\mu$. Consider a spherical droplet of phase β with radius R^*, much

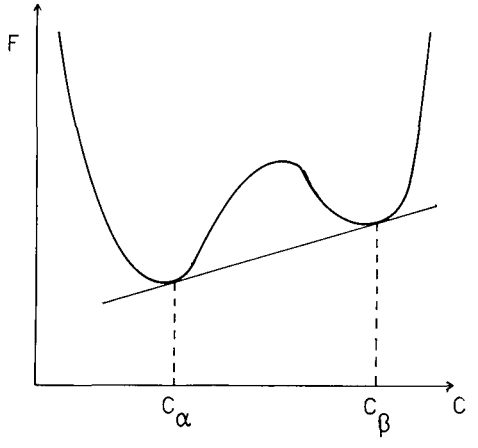

FIGURE 1
Typical coarse-grained free-energy density f(c). Also shown is the common-tangent construction mentioned in the text.

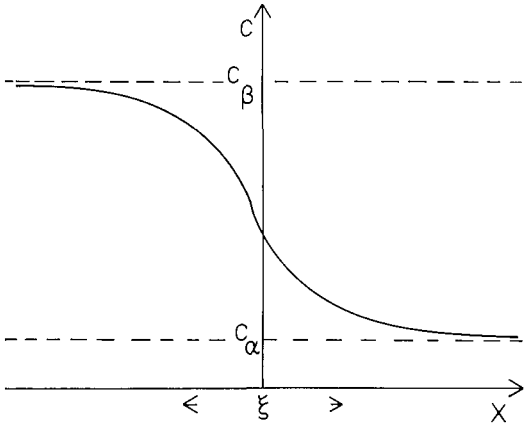

FIGURE 2
Sketch of the density profile c(x) at a planar interface between phases α and β. The length ξ measures the width of the interfacial layer.

larger than the interfacial scale ξ. Instead of eq. (2.6) we now have for the radial density distribution c(r) the equation (taking r = 0 at the center of the droplet)

$$\frac{df}{dc} - K\left(\frac{d^2c}{dr^2} + \frac{2}{r}\frac{dc}{dr}\right) = \mu, \tag{2.7}$$

which may be written in the equivalent form

$$-\frac{d}{dr}\left[\frac{1}{2}K\left(\frac{dc}{dr}\right)^2 + \mu c - f\right] = \frac{2}{r}K\left(\frac{dc}{dr}\right)^2. \tag{2.8}$$

Integrating both sides over a small interval of order ξ around R^*, we find to linear order in the supersaturation $\delta\mu$ (i.e. neglecting the dependence of δc on $\delta\mu$)

$$\delta\mu\ \delta c = 2\sigma/R^*, \text{ with } \sigma \equiv K\int dr\ \left(\frac{dc}{dr}\right)^2. \tag{2.9}$$

This relation between supersaturation and interfacial curvature is a special form of the Gibbs-Thomson relation. It expresses the fact that small droplets are in equilibrium with a higher solute concentration than large droplets. The quantity σ defined above can be identified as the surface energy per unit area, or surface *tension*.

The Gibbs-Thomson relation (2.9) may also be obtained from the expression for the free energy of formation $\Delta F(R)$ of a droplet of radius R,

$$\Delta F(R) = -\frac{4}{3}\pi R^3 \delta\mu\ \delta c + 4\pi R^2\sigma, \tag{2.10}$$

which consists of a bulk part which favors the formation (for positive $\delta\mu$) and a part representing the surface energy which has the opposite effect. Fig. 3 shows the typical free-energy barrier which must be overcome for nucleation to occur. The stationary state can be found by equating to zero the first deriva-

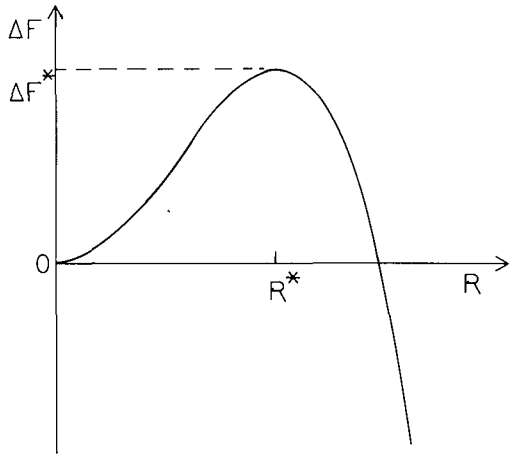

FIGURE 3
Free energy of formation ΔF of a droplet of radius R. The maximum of the curve locates the (unstable) stationary state.

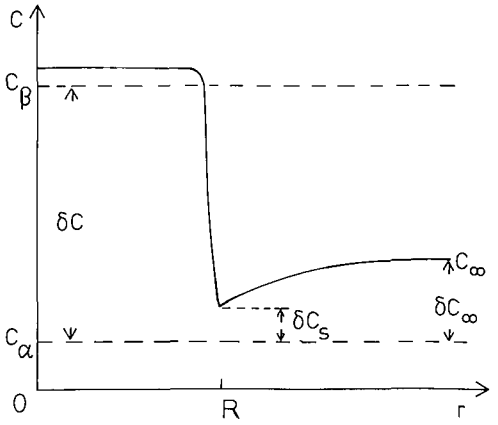

FIGURE 4
Sketch of the radial density distribution c(r) for a spherical droplet, showing various quantities defined in the text.

tive of $\Delta F(R)$ and turns out to be given precisely by eq. (2.9), as it should. Note that this state corresponds to a *maximum* of the free energy, and is therefore an *unstable* stationary state. The activation energy $\Delta F^* \equiv \Delta F(R^*)$ is found to be

$$\Delta F^* = \frac{16}{3}\pi\sigma^3(\delta\mu\ \delta c)^{-2}. \tag{2.11}$$

As a consequence of the inverse square dependence of the activation energy on deviations of the chemical potential from its equilibrium value, measurements of nucleation rates are extremely sensitive for small variations in the degree of supersaturation. Indeed, this rate depends on ΔF^* exponentially as[14] $\exp(-\Delta F^*/k_BT)$ (where k_B and T are, respectively, Boltzmann's constant and the temperature) and therefore a small variation of, say, 10% in the supersaturation can change the nucleation rate by a factor 10^6! Conversely, experiments are not very sensitive for the precise value of the coefficient of the exponential (which for fluids is of the order of 10^{30} droplets/cm^{3}s). For very recent direct measurements of nucleation rates in well-defined systems we refer to refs. 15 and 16.

3. KINETICS OF DROPLET GROWTH

Once droplets of the new phase β have formed, their growth is generally controlled by a diffusive process which takes place on a macroscopic length scale, much larger than the interfacial scale ξ. In this case we may assume that the chemical potential is approximately constant over the interface, equal to say $\mu_c + \delta\mu_s$, and is related to the droplet radius R by the Gibbs-Thomson relation (2.9). We consider first the growth of a single droplet.

The concentration of phase α just outside the droplet equals $c_\alpha + \delta c_s$, where δc_s is the deviation of this concentration from the value c_α corresponding to a planar interface (cf. fig. 4). To linear order in $\delta\mu_s$ we may write $\delta c_s = \chi_\alpha \delta\mu_s$, with a susceptibility $\chi_\alpha \equiv \partial c_\alpha/\partial\mu$. (For an ideal - i.e. sufficiently dilute - solution, $\chi_\alpha = c_\alpha/k_BT$.) Together with eq. (2.9) we then find

$$\delta c_s = 2\sigma\chi_\alpha(R\ \delta c)^{-1}. \tag{3.1}$$

The radial concentration distribution c(r,t) outside the droplet (with radius R(t) and center at r = 0) may be obtained by solving the diffusion equation (2.5) in the *quasi-static* approximation,

$$0 = D\nabla^2 c(r,t)\ \left(= D\,\frac{1}{r}\,\frac{\partial^2}{\partial r^2}\,rc(r,t)\right), \tag{3.2}$$

where D is the diffusion coefficient of the α-phase. (For a justification of the neglect of the time-derivative of c in eq. (2.5), see below.) With the boundary conditions

$$\lim_{r\downarrow R(t)} c(r,t) = c_\alpha + \delta c_s,\quad \lim_{r\to\infty} c(r,t) = c_\alpha + \delta c_\infty \equiv c_\infty, \tag{3.3}$$

eq. (3.2) has the solution

$$c(r,t) = c_\infty - \frac{R(t)}{r}\,(\delta c_\infty - \delta c_s). \tag{3.4}$$

If the concentration c_∞ far from the droplet differs from the concentration at the interface there is a non-zero diffusion current $D\partial c/\partial r$, which causes the droplet to grow (or shrink) with radial velocity $V(t) \equiv dR(t)/dt$ given by

$$V(t) = (\delta c)^{-1}\,D\,\frac{\partial c(r,t)}{\partial r}\Big|_{r=R} \tag{3.5}$$

(where we have again neglected the dependence of δc on $\delta\mu$). Substituting eq. (3.4) into eq. (3.5) we thus find

$$V = D(R\delta c)^{-1}(\delta c_\infty - \delta c_s) = \frac{D}{r}(\Delta - 2d_0/R), \tag{3.6}$$

where we have introduced the dimensionless supersaturation $\Delta \equiv \delta c_\infty/\delta c$ and the capillary length $d_0 \equiv \sigma\chi_\alpha/(\delta c)^2$ (which is a microscopic quantity, of the same order of magnitude as ξ). In terms of these two quantities the critical radius R^* at which the droplet is in a stationary state (i.e., $V = 0$) is given by $R^* = 2d_0/\Delta$.

The above results are based on the quasi-static approximation (3.2) of the diffusion equation (2.5). This approximation is justified if the time in which a molecule diffuses over a distance R (which time is of the order of R^2/D) is much smaller than R/V, which is the time in which a droplet grows by an appreciable fraction of its radius. That is, we require $R \ll D/V$, or $\Delta \ll 1$.

To conclude this analysis of the growth of an isolated droplet, we observe that eq. (3.6) implies that the radius R(t) grows as $\sqrt{(2Dt)}$ for large times (i.e. for $R \gg R^*$). This growth law will change when the diffusion fields of many droplets overlap, and in fact it turns out that the average radius $\bar{R}$ of the droplets increases *asymptotically* with the cubic, rather than the square, root of time. More precisely, the Lifshitz-Slyosov[17] and Wagner[18] theory of diffusion controlled competitive growth predicts that, independent of initial conditions,

$$\bar{R} \to R^* \to (\frac{8}{9} d_0 Dt)^{1/3}, \text{ as } t \to \infty. \tag{3.7}$$

We shall now investigate this asymptotic time dependence, and in particular the way of approach to the asymptote, by a very simple theory[19], which allows us to obtain a great deal of information with a minimum amount of mathematical analysis.

We first define a droplet-size distribution function $\nu(R,t)$, such that $\nu(R,t)dR$ gives the average number density at time t of droplets with radii between R and R + dR. From now on we shall neglect nucleation of droplets, which one can justify on grounds of the exponential decline of the nucleation rate with decreasing supersaturation (see the previous section). (For theories which include both growth and nucleation, we refer to refs. 19 and 20.) The function $\nu(R,t)$ then satisfies the continuity equation

$$\frac{\partial \nu(R,t)}{\partial t} = -\frac{\partial}{\partial R} i(R,t), \tag{3.8}$$

with a current $i(R,t)$. We now take the "effective medium" approximation by putting $i(R,t)$ equal to $V(R,t)\nu(R,t)$, where $V(R,t)$ is the growth velocity (3.6) of a single droplet with radius R in a medium with supersaturation $\Delta(t)$. This *effective* supersaturation is time dependent and must be determined as part of the problem, selfconsistently. In terms of the critical radius $R^*(t) = 2d_0/\Delta(t)$ we therefore write for $i(R,t)$

$$i(R,t) = 2d_0 DR^{-1}(R^*(t)^{-1} - R^{-1})\nu(R,t). \tag{3.9}$$

Next we define the total number density of droplets in the condensate N(t)

$$N(t) = \int_{R^*(t)}^{\infty} \nu(R,t)dR \tag{3.10}$$

and the average radius $\bar{R}(t)$

$$\bar{R}(t) = N(t)^{-1} \int_{R^*(t)}^{\infty} \nu(R,t)RdR. \tag{3.11}$$

In these equations we have taken the convention of counting only supercritical droplets as part of the condensate, hence the lower limit of integration at $R^*(t)$. (This device - if supplemented by a certain *ad hoc* closure assumption given below - will allow us to deal with only the above first two moments of $\nu(R,t)$. The complete asymptotic distribution function has been derived by Lifshitz and Slyosov[17].) Using eqs. (3.8) and (3.9) we find the two equations of motion (omitting the time arguments of all quantities)

$$\frac{dN}{dt} = - \nu(R^*) \frac{dR^*}{dt} , \tag{3.12}$$

$$\frac{d\bar{R}}{dt} \approx 2d_0 D(\bar{R})^{-1}((R^*)^{-1} - (\bar{R})^{-1}) + \nu(R^*)N^{-1}(\bar{R} - R^*) \frac{dR^*}{dt} . \tag{3.13}$$

In the first term on the r.h.s. of eq. (3.13) we have approximated the average over the droplet-size distribution function of $V(R)$ by $V(\bar{R})$, assuming a distribution which is not too broad.

Our final equation relates the current supersaturation $\Delta(t)$ to the volume fraction of the condensate,

$$\Delta_0 - \Delta = \frac{4}{3} \pi \overline{(R^3)} N \approx \frac{4}{3} \pi (\bar{R})^3 N, \tag{3.14}$$

where Δ_0 is the initial supersaturation, in the absence of condensed droplets. Eq. (3.14) expresses (to linear order in Δ) the conservation of the number of molecules. We note that, as a result of our definition of N and $\bar{R}$, *sub*critical droplets are considered to contribute to the supersaturation. We feel that this is not too serious an inconsistency.

To close the set of equations (3.12)-(3.14) we still need an estimate for $\nu(R)$ at $R = R^*$. A reasonable choice seems

$$\nu(R^*) = bN(\bar{R} - R^*)^{-1}, \tag{3.15}$$

with an as yet unspecified numerical constant b. The above eqs. (3.12)-(3.15) give both $\bar{R}$ as a function of R^* and R^* as a function of t.

First, combining eqs. (3.12), (3.14) and (3.15) we find a differential equation for $\bar{R}(R^*)$, for given initial critical radius $R_0^* \equiv 2d_0/\Delta_0$,

$$d\bar{R}/dR^* = \frac{1}{3} (\bar{R}/R^*)(R^*/R_0^* - 1)^{-1} + \frac{b}{3} \bar{R}(\bar{R} - R^*)^{-1}. \tag{3.16}$$

For $R^* >> R_0^*$ the first term on the r.h.s. of this equation may be neglected and one finds the solution

$$\bar{R} - (1 + b/3)R^* = \text{constant} \times (\bar{R})^{-3/b}. \tag{3.17}$$

As we see, $\bar{R}(R^*)$ has an asymptote $\bar{R} = (1 + b/3)R^*$, for large $\bar{R}$. That this asymptotic behaviour differs somewhat from the Lifshitz-Slyosov and Wagner result (3.7) is due (in part) to our convention of averaging only over supercritical droplets in eqs. (3.10) and (3.11). Typical trajectories of eq. (3.16) (for the value of b given below) are shown in fig. 5.

Next, eqs. (3.13) and (3.15) together with the approximation $\bar{R} \approx (1+b/3)R^*$, give the equation for the asymptotic time-evolution of $R^*(t)$

$$\frac{d}{dt} (R^*)^3 \approx 2b(1 + b/3)^{-2}(1 - 2b/3)^{-1} d_0 D. \tag{3.18}$$

We see that R^* increases as $t^{1/3}$, in agreement with eq. (3.7). The correct coefficient is recovered if we put $b \approx 0.42$.

We can distinguish two qualitatively different ways of approach to the asymptotes. The trajectory labeled S in fig. 5 can be interpreted as corresponding to the case of a "shallow quench", where - because the droplets remain

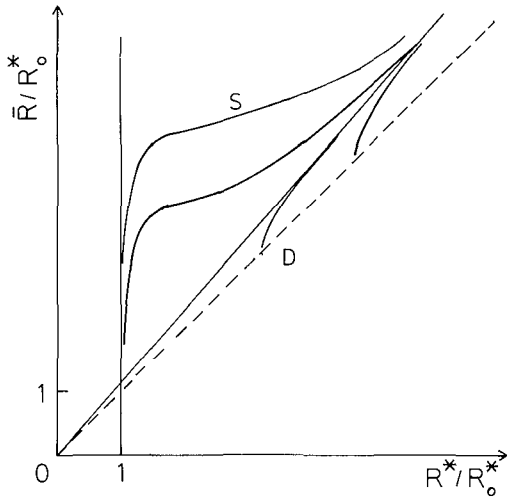

FIGURE 5
Some trajectories of eq. (3.16) (for b=0.42). The unphysical parts of the solutions are dotted. Both the cases of a shallow quench (curve S) and a deep quench (curve D) are shown.

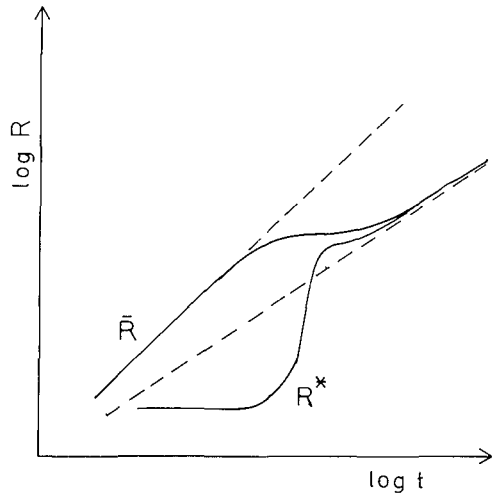

FIGURE 6
Sketch of the time dependence of the average radius $\bar{R}$ and the critical radius R^* for a shallow quench. The two dashed asymptotes correspond to the growth laws $R \propto t^{1/2}$ and $R \propto t^{1/3}$.

isolated for a long time - the average radius $\bar{R}$ can grow much larger than R^*, before approaching its asymptote. For a "deep quench", on the other hand, there is an initial high density of small droplets and competition effects are important at early stages of the droplet growth. In this case the approach to the asymptote is rapid (cf. trajectory D in fig. 5). The dependence of $\bar{R}$ and R^* on t for a shallow quench is sketched in fig. 6, to illustrate the above remark.

The effective medium theory for competitive growth described here can be improved considerably by taking into account the effect of correlations between the positions and sizes of the droplets[21 22 23], and the influence of nucleation[19 20]. Nevertheless, our qualitative results for the approach to the Lifshitz-Slyosov and Wagner asymptotes have their use in the interpretation of experimental data, in particular in determining the regime in which the $t^{1/3}$-growth law is expected to hold.

4. GROWTH INSTABILITIES AND PATTERN FORMATION

4.1. Morphological instability of a growing spherical droplet

As an initially spherical droplet grows, its shape will eventually become unstable against perturbations of a sufficiently long wavelength. The critical wavelength at which this morphological instability occurs is determined by a balance between, on one hand, the destabilizing effect of the focusing of diffusion flux away from a depression of the interface onto a protuberance (in a way, a protuberance acts as a lightning rod) and, on the other hand, the stabilizing effect of surface tension, which favors a smooth spherical interface. An analogous instability occurs, by the way, during the solidification of a pure substance from its undercooled melt, where the increase in the rate at which latent heat is released at a protuberance of the solidification front

is the destabilizing factor. The onset of these growth instabilities has been studied by Mullins and Sekerka[24] [25]. We shall now give an outline of their linear stability analysis.

Consider a slightly deformed spherical droplet growing under the conditions of section 3. The distance R of the interface to the origin is given, in terms of the polar angles Θ and ϕ, by

$$R(\Theta,\phi,t) = R_0(t) + \sum_{\ell\geq 1;m} R_\ell(t) Y_{\ell m}(\Theta,\phi). \tag{4.1}$$

Here R_0 is the unperturbed radius, R_ℓ ($\ell\geq 1$) is a small deformation amplitude and $Y_{\ell m}$ is the spherical harmonic of order ℓ,m . To determine the concentration field we shall again use the quasi-static approximation (3.2) of the diffusion equation. (The consistency of this approximation in connection with the present stability analysis is investigated below.) The dimensionless solution $u(\vec{r},t) \equiv (c_\infty - c(\vec{r},t))/\delta c$ of this equation (outside the droplet) has the expansion

$$u(\vec{r},t) = \sum_{\ell\geq 0;m} a_\ell(t) r^{-\ell-1} Y_{\ell m}(\Theta,\phi), \quad r > R(\Theta,\phi). \tag{4.2}$$

The coefficients a_ℓ ($\ell\geq 0$) are determined by the boundary condition for the concentration field at the interface, which is the Gibbs-Thomson relation for a non-spherical surface,

$$\lim_{r\downarrow R(\Theta,\phi)} u(\vec{r},t) = \Delta - d_0\kappa(\Theta,\phi,t). \tag{4.3}$$

Here κ is the mean curvature of the interface, which to linear order in the deviation from sphericity equals[24]

$$\kappa = 2/R_0 + R_0^{-2} \sum_{\ell\geq 2;m} (\ell-1)(\ell+2) R_\ell Y_{\ell,m}. \tag{4.4}$$

Substituting eq. (4.2) into eq. (4.3) gives, with eq. (4.4), the required result

$$a_0 = R_0\Delta - 2d_0, \quad a_\ell = R_0^{\ell-1} R_\ell (R_0\Delta - d_0\ell(\ell+1)) \quad (\ell\geq 1). \tag{4.5}$$

To investigate the stability of the spherical shape we must determine whether the deformation amplitudes $R_\ell(t)$ ($\ell\geq 1$) grow or decay in time. To this end we substitute the concentration field given by eqs. (4.2) and (4.5) into the equation of motion of the interface (3.5),

$$\frac{d}{dt} R_0(t) + \frac{d}{dt} \sum_{\ell\geq 1;m} R_\ell(t)\, Y_{\ell m}(\Theta,\phi) = - D \frac{\partial}{\partial r} u(\vec{r},t)\Big|_{r=R(\Theta,\phi)} . \tag{4.6}$$

The result is

$$dR_0/dt = DR_0^{-1}(\Delta - 2d_0/R_0) \equiv V_0, \tag{4.7}$$

where V_0 is the growth velocity (3.6) of a perfect sphere, and

$$R_\ell^{-1}\, dR_\ell/dt \equiv \omega_\ell = (\ell-1)V_0R_0^{-1}[1 - (\ell+1)\ell+2)R_0^{-2}d_0D/V_0]. \tag{4.8}$$

The sign of the growth rate ω_ℓ determines the stability of the spherical shape against a harmonic perturbation $Y_{\ell m}$.

Eq. (4.8) takes a particularly simple form in the limit of perturbations of a finite lengthscale 1/k on a large sphere, that is in the limit

$R_0 \to \infty$, $\ell \to \infty$, $\ell/R_0 \equiv k$ = constant. In this socalled planar limit the growth rate $\omega(k) \equiv \omega_{\ell=R_0 k}$ is given by

$$\omega(k) = V_0 k(1 - k^2 d_0 D/V_0). \tag{4.9}$$

As we see, the planar interface is unstable for all perturbations of length-scale larger than $\surd(d_0 D/V_0)$. This characteristic stability length is of order microns and is the geometric mean of the *microscopic* capillary length d_0 and the *macroscopic* diffusion length D/V_0.

At this point we can check the consistency of the quasi-static approximation. The criterion for the validity of this approximation in the present context is that the diffusive relaxation rate Dk^2 is much larger than the magnitude $|\omega(k)|$ of the growth rate (cf. section 3). From eq. (4.9) we find that this criterion is satisfied in the range $V_0/D \ll k \ll 1/d_0$. The maximum of $\omega(k)$, which falls at $k = \surd(V_0/3d_0 D)$, lies in this range, so that the quasi-static approximation holds in particular for the growth of the dominant instability. (There exist physically interesting models for which this is not true, however.)

Returning to eq. (4.8), let us now compute the radius R_ℓ^c at which the sphere becomes unstable for a harmonic perturbation of order ℓ. Equating ω_ℓ to zero in eq. (4.8) gives, in terms of the critical radius for nucleation $R^* = 2d_0/\Delta$,

$$R_\ell^c/R^* = 1 + \frac{1}{2}(\ell+1)(\ell+2) \quad (\ell \geq 2). \tag{4.10}$$

The first instability occurs for ℓ=2, thus a sphere of radius $R_0 = 7R^*$ is unstable†. Spheres of this size are really quite small, typically in the submicron range. Note, however, that - if capillarity is neglected - a sphere perturbed by only the second harmonic does not change shape as it grows. This can most easily be seen by looking at eqs. (4.7) and (4.8) which give, in the limit $R_0 \gg R^*$,

$$dR_\ell/dR_0 = (\ell-1)R_\ell/R_0. \tag{4.11}$$

Thus for $\ell = 2$, the fractional rate of increase of the deformation amplitude is equal to that of the radius of the sphere.

4.2. Dendritic growth

What happens to a growing droplet after its spherical shape has become unstable? It is observed that an initially spherical interface breaks up into *dendritic*, i.e. treelike, branches which grow out from the central "seed", each branch emitting sidebranches as it grows. The dendritic solidification of a pure substance from its undercooled melt has been investigated under carefully controlled experimental conditions by Glicksman and coworkers[26 27] (who used succinonitrile as a working substance) and by Fujioka[28 29] (using ice). It is found that the growth velocities and shapes of the frontmost tips of the primary branches, as well as the spacings of emerging sidebranches, are accurately reproducible functions of the undercooling (which is the parameter

†Note that ω_ℓ for $\ell = 1$ is identically zero, for all R_0. Indeed the first harmonic merely translates the sphere over a small distance.

which plays in this context the role of the supersaturation†). There is to date no complete theory which predicts the undercooling dependence of these quantities. However, some progress has been made in recent years, resulting in an hypothesis which - if valid - permits one to use the results of a linear stability analysis to predict dendritic growth rates[30]. We summarize below the arguments leading to this hypothesis.

Consider, as a simple model of a dendrite, a solidification front which is a paraboloid of circular cross-section. We look for solutions of the problem which are time-independent with respect to a frame of reference which moves with a certain constant growth velocity V. If one assumes that the radius of curvature R of the tip is sufficiently large compared to d_0 that surface-tension effects may be neglected, then such shape-preserving solutions may be determined exactly, as shown by Ivantsov[31]. The result of interest here is

$$\Delta = pe^p \int_p^\infty y^{-1}e^{-y}dy \quad \approx \quad \begin{cases} -p\ell np & \text{if } p \ll 1, \\ 1 - 1/p & \text{if } p \gg 1, \end{cases} \tag{4.12}$$

where $p \equiv RV/2D$ is the socalled thermal Péclet number. (For later reference we record here also the corresponding two-dimensional result,

$$\Delta\ (\textit{two-dimensions}) = 2e^p\sqrt{p}\int_{\sqrt{p}}^\infty e^{-y^2}dy \quad \approx \quad \begin{cases} \sqrt{(\pi p)} & \text{if } p \ll 1, \\ 1 - \frac{1}{2}p^{-1} & \text{if } p \gg 1.) \end{cases} \tag{4.13}$$

For a given value of Δ there is a whole family of solutions, as only the product of tip radius and growth velocity is fixed by eq. (4.12). The R-V plot for $\Delta = 0.05$ is shown in fig. 7.

As we have learned from our study of a growing sphere (cf. eq. (3.6)), the effect of surface tension - not included in eq. (4.12) - is to reduce the growth velocity for large values of the curvature, i.e. for small tip radii. To determine quantitatively, however, the effect of surface tension on the steady state growth of the dendrite turns out to be extremely difficult (and in fact, as we shall argue in sub-section 4.3, there is reason to suspect that the picture which has emerged from various approximate analyses will have to be modified). The results of two of these approximations[32 33] are shown in fig. 7. Due to surface-tension effects V goes through a maximum with decreasing R. (The location of this maximum has been estimated by an alternative, numerical, technique in ref. 34.) Which of these solutions are stable against small shape deformations? One would expect for sufficiently large tip radii a morphological instability of the Mullins-Sekerka type to occur, as in the spherical case discussed previously. Indeed it is found[30], from a linear stability analysis in the regime $p \ll 1$, that a sufficiently flat tip becomes unstable against deformations in which the tip breaks up into sharper, more rapidly growing protuberances. The criterion for stability is $d_0D/VR^2 > \sigma^*$,

†The full translation from chemical to thermal diffusion is made by replacing the definitions of u, Δ and d_0 given previously for the chemical case by

$u \equiv (T - T_\infty)c_p/L$, $\Delta \equiv (T_m - T_\infty)c_p/L$ and $d_0 \equiv \sigma T_m c_p/L^2$.

Here, T is the local temperature, T_m the melting temperature at a planar interface, T_∞ the temperature in the liquid infinitely far from the region where solidification is taking place, c_p is the isobaric specific heat and L the latent heat, both per unit volume. Also, D should now be regarded as the thermal diffusion coefficient of the liquid. Note, however, that one must in general account also for thermal diffusion within the solid, in contrast to the chemical case.

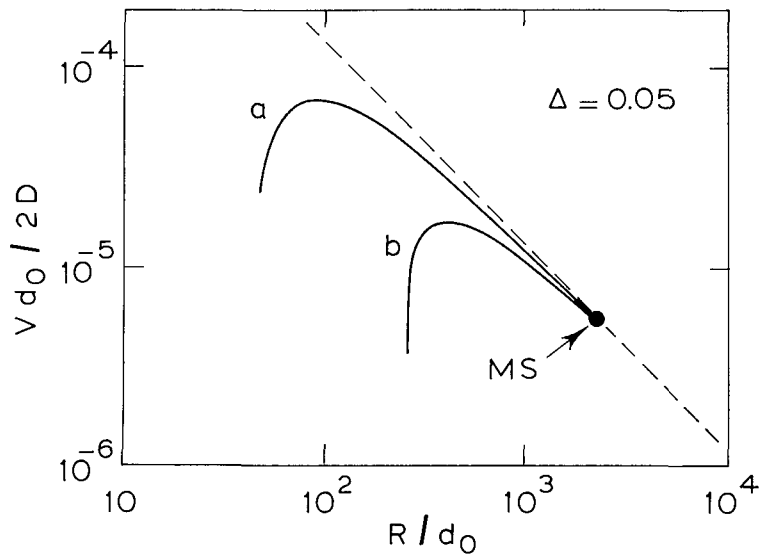

FIGURE 7
Dendritic growth velocity versus tip radius for the undercooling $\Delta = 0.05$. The dashed curve is the exact result[31] without surface tension (eq. 4.12). Curves a (from ref. 32) and b (from ref. 33) result from two different approximations of the effect of surface tension. The point of marginal stability of the solutions with surface tension for the case of succinonitrile[30] is labeled MS.

where σ^* is a constant whose value is estimated at 0.02 for succinonitrile. The point of marginal stability, for which the equality in the above criterion holds, is plotted in fig. 7 for this value of σ^*.

So far we are still left with a continuous family of solutions, all of which are acceptably stable candidates for the description of dendritic growth at a given undercooling. In fact we surmise that the mechanism by which definite R and V are selected is of an intrinsically non-linear mechanical nature, and can therefore not be obtained from the linear analysis dicussed above. A selection principle for dendritic growth, which has been used with considerable succes in various applications, is the *principle of marginal stability* suggested by Langer and Müller-Krumbhaar in ref. 30. In that paper it is conjectured that an initially smooth, unstable shape might naturally sharpen until it reaches its slowest stable growth mode. In other words, the natural operating mode of the dendrite is presumed to be at or near the growth rate where its tip is just marginally stable. This principle, together with the results from the linear stability analysis[30], has proved to be consistent with experimental data[26 27 28 29] over five decades in the growth velocity and two in the undercooling. (As an aside, we note that this principle has also correctly predicted the - at first surprising - initial *rise* in growth velocity that occurs when small concentrations of impurities are added to the melt, the point being that the impurity layer has a destabilizing effect on the solidification front, thus leading to sharper and faster dendritic structures[35 36 37].)

4.3. The boundary-layer model

Because of the complexity of the full dendritic solidification problem described above, progress in understanding the observed growth-selection mechanisms has been very slow. In particular we do not know from a theoretical point of view what is the validity of the marginal-stability hypothesis. One of the aspects of the full problem which apparantly make it so intractable is the non-locality of the equations in both space and time. That is to say, the actual motion of a point on a solidification front is determined by the thermal field near that point which, in turn, is determined by the latent heat which has been generated at earlier times at neighbouring points. The boundary-layer model[38] which we shall now describe is a tractable, fully non-linear mathematical model of solidification at large undercoolings, in which the non-locality is accounted for only approximately via the properties of a supposedly thin thermal boundary layer at the interface.

The principal dynamical variables in the boundary-layer model are the curvature of the solidification front κ and a new variable h, which is supposed to measure the heat content per unit area of a thermal layer in the liquid which contains the latent heat that has been rejected by the advancing solid. Both quantities κ and h are functions of the time t and the position along the interface. For simplicity, we shall restrict ourselves here to a two-dimensional situation (cf. fig. 8) and measure the linear position along the interface by the arc length s. Knowing κ as a function of s, it is possible to reconstruct the entire shape of the growing solid.

If we define the two-dimensional curvature by

$$\kappa = - \partial\theta/\partial s, \tag{4.14}$$

it satisfies the geometric identity[39]

$$\left(\frac{d\kappa}{dt}\right)_n = - \left(\kappa^2 + \frac{\partial^2}{\partial s^2}\right) V_n. \tag{4.15}$$

Here θ is the angle between the normal to the interface and some arbitrarily fixed direction in space, V_n is the normal growth rate of the front and $(d/dt)_n$ denotes the rate of change along the normal growth direction. A suitable equation of motion for the second field h is

$$\left(\frac{dh}{dt}\right)_n = V_n(1 - u_s) + D \frac{\partial}{\partial s}\left(\ell \frac{\partial}{\partial s} u_s\right) - hV_n\kappa, \tag{4.16}$$

where u_s is the value of the dimensionless temperature field u at the interface (cf. the previous footnote) and $\ell \equiv h/u_s$ is the effective thickness of the thermal boundary layer. The first term on the r.h.s. of eq. (4.16) is the rate at which latent heat is being added to the boundary layer, the second term accounts for lateral diffusion of this heat along the surface (it is by this diffusion term that some of the non-local features of the realistic dynamics are incorporated into this local model); the third term is a geometrical correction, which can be identified as the origin of the Mullins-Sekerka instability: a surface element of positive curvature (outward bulge) increases in length as it grows, thus thinning the boundary layer, sharpening the thermal gradient, and increasing the growth rate.

The two above equations of motion are supplemented by expressions for u_s and V_n,

$$u_s = \Delta - d_0\kappa - \beta V_n, \tag{4.17}$$

$$V_n = Du_s/\ell \quad \left(= Du_s^2/h\right). \tag{4.18}$$

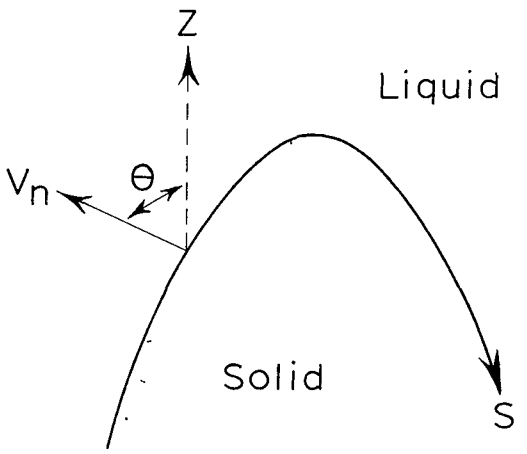

FIGURE 8
Schematic illustration of a solidification front, showing various quantities defined in the text.

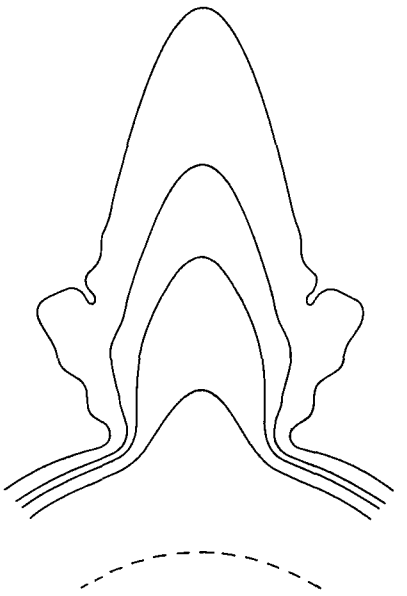

FIGURE 9
Evolution of a dendritelike structure, from the boundary-layer model.

Eq. (4.17) is just the Gibbs-Thomson relation, with the addition of the term $-\beta V_n$ which follows from a simple model of interfacial attachment kinetics. The capillary length d_0 and the kinetic coefficient β may be functions of Θ, reflecting a possible crystalline anisotropy. In eq. (4.18), heat flow in the solid is neglected and the normal temperature gradient in the fluid is approximated by u_S/ℓ.

Physical validity of the boundary-layer model described above requires that the boundary layer be thin compared to the radius of curvature of the solidification front. In general, this condition is satisfied only at large Peclet numbers. Although this regime is physically accessible in principle, most experiments (in particular those on dendritic growth mentioned previously) are performed in the regime of small undercoolings and Peclet numbers. In any case, even under circumstances where the model is not fully realistic, it turns out to be an interesting mathematical model of pattern selection.

As an example[38], let us apply the boundary-layer model to the dendrite problem and compare the results from this model with those from the analyses discussed in sub-section 4.2. To this end we look for a solution of eqs. (4.15)-(4.18) such that

$$V_n = V_0 \cos\Theta, \tag{4.19}$$

$$\left(\frac{dh}{dt}\right)_\Theta \equiv \left(\frac{dh}{dt}\right)_n + \kappa \frac{\partial V_n}{\partial \Theta} \frac{\partial h}{\partial \Theta} = 0. \tag{4.20}$$

The vanishing of the derivative at constant Θ in eq. (4.20) expresses the requirement that the h-field remain invariant in the frame of reference which moves with the constant growth velocity V_0 in, for example, the z-direction in fig. 8 . The relative simplicity of the boundary-layer method is apparent in

the fact that we can use eqs. (4.17)-(4.19) to eliminate h from the problem, thus obtaining a single non-linear differential equation for κ as a function of Θ (which is the convenient independent variable for this problem, rather than s).

For the case $d_0 = \beta = 0$ one finds the simple result

$$\kappa(\Theta) = (V_0/D)(1 - \Delta)\Delta^{-2}\cos^3\Theta, \tag{4.21}$$

which is a parabola with its tip pointing in the +z - direction. The tip-radius is $1/\kappa(0)$. Thus, in terms of the Péclet number $p = V_0/2D\kappa(0)$, we have the formula

$$p = \frac{1}{2}\Delta^2(1 - \Delta)^{-1} \quad \approx \quad \begin{cases} \sqrt{(2p)} & \text{if } p \ll 1, \\ 1 - \frac{1}{2}p^{-1} & \text{if } p \gg 1. \end{cases} \tag{4.22}$$

The large-p limit of eq. (4.22) is identical to the exact Ivantsov-result[31] (eq. 4.13) for this two-dimensional case. Surprisingly, the (unrealistic) small-p limit of eq. (4.22) also compares very well with that of eq. (4.13). (A similar analysis has been performed in three dimensions as well[38], to yield $p = \Delta^2/(1 - \Delta)$. There is now a more serious discrepancy with the exact result (4.12) in the small-p limit, although the large-p behaviour is again correct.)

What happens if we include surface-tension effects in our equations of motion? We shall not go into the analysis[38] here, but only mention the surprising result: in the boundary-layer model, surface-tension corrections give a *singular* perturbation of the $d_0 = 0$ solution, destroying the continuous family of shape-preserving solutions found in the absence of surface tension. This result casts serious doubts on the validity of the various approximate solutions to the full dendritic solidification problem at finite d_0, discussed in the previous sub-section.

Finally, we show in fig. 9 four (not quite evenly spaced) stages in the growth of a dendritic structure, computed from the boundary-layer model with a six-fold anisotropy in the kinetic coefficient β. The structure started as a circle (one sixth of which is indicated by the dashed line), grew slowly almost into a hexagon, and then became dendritic at its corners as shown. The growth rate and the curvature of the front of this dendrite have relaxed quickly to their dynamically selected steady-state values.

REFERENCES

1) Much of the material in these lectures is treated more extensively in the following two recent reviews:
   J.D. Gunton, M. San Miguel and P.S. Sahni, The Dynamics of First-Order Phase Transitions, in: Phase Transitions and Critical Phenomena, Vol. 8, eds. C. Domb and J.L. Lebowitz (Academic Press, New York, 1983);
   J.S. Langer, Rev. Mod. Phys. 52 (1980) 1.
2) J.D. van der Waals, Verhandel. Konink. Akad. Weten. Amsterdam, Sect. 1, 1 (1893) No. 8; for an English translation see:
   J.S. Rowlinson, J. Stat. Phys. 20 (1979) 197.
3) J.S. Rowlinson and B. Widom, Molecular Theory of Capillarity (Clarendon Press, Oxford, 1982).
4) J.W. Cahn and J.E. Hilliard, J. Chem. Phys. 28 (1958) 258.
5) S. Fisk and B. Widom, J. Chem. Phys. 50 (1969) 3219.
6) N.G. van Kampen, Phys. Rev. 135A (1964) 362.
7) J.S. Langer, Physica 73 (1974) 61.
8) J.W. Cahn, Metastability, Instability, and the Dynamics of Unmixing in Binary Critical Systems, in: Critical Phenomena in Alloys, Magnets, and Superconductors, eds. R.I. Jafee, R.E. Mills and E. Ascher (McGraw-Hill, New York, 1971).

9) J.E. Hilliard, Spinodal Decomposition, in: Phase Transformations, ed. H.I. Aronson (Am. Soc. for Metals, Metals Park, Ohio, 1970).
10) J.S. Langer, Ann. Phys. 54 (1969) 258; 65 (1971) 53.
11) J. Frenkel, Kinetic Theory of Liquids (Dover, New York, 1955).
12) A.C. Zettlemoyer ed., Nucleation (M. Dekker, New York,1969).
13) F.F. Abraham, Homogeneous Nucleation Theory (Academic Press, New York, 1974).
14) E.M. Lifshitz and L.P. Pitaevskii, Physical Kinetics (Pergamon, Oxford, 1981) ch. XII.
15) E.D. Siebert and C.M. Knobler, Phys. Rev. Lett. 52 (1984) 1133.
16) H. Wendt and P. Haasen, Acta Metall. 31 (1983) 1649.
17) I.M. Lifshitz and V.V. Slyosov, Phys. Chem. Solids 19 (1961) 35; an extensive discussion of this theory is given in ref. 14.
18) C. Wagner, Z. Elektrochem. 65 (1961) 581.
19) J.S. Langer and A.J. Schwartz, Phys. Rev. 21A (1980) 948.
20) K. Binder and D. Stauffer, Adv. Phys. 25 (1976) 343.
21) K. Tsumuraya and Y. Miyata, Acta Metall. 31 (1983) 437, and refs. therein.
22) A.D. Brailsford and P. Wynblatt, Acta Metall. 27 (1979) 489.
23) J.A. Marqusee and J. Ross, J. Chem. Phys. 80 (1984) 536.
24) W.W. Mullins and R.F. Sekerka, J. Appl. Phys. 34 (1963) 323; 35 (1964) 444.
25) R.F. Sekerka, Morphological Stability, in: Crystal Growth, an Introduction, ed. P. Hartman (North-Holland, Amsterdam, 1973).
26) M.E. Glicksman, R.J. Shaefer and J.D. Ayers, Metall. Trans. 7A (1976) 1747.
27) S.C. Huang and M.E. Glicksman, Acta Metall. 29 (1981) 701; 717.
28) T. Fujioka, Ph.D. Thesis, Carnegie-Mellon Univ., Pittsburgh (1978).
29) J.S. Langer, R.F. Sekerka and T. Fujioka, J. Crystal Growth, 44 (1978) 414.
30) J.S. Langer and H. Müller-Krumbhaar, Acta Metall. 26 (1978) 1681; 1689; 1697.
31) G.P. Ivantsov, Dokl. Akad. Nauk. SSSR 58 (1947) 567.
32) R.F. Sekerka, R.G. Seidensticker, D.R. Hamilton and J.D. Harrison, Investigation of Desalination by Freezing, Westinghouse Research Laboratory Report (1967), Chap. 3.
33) D.E. Temkin, Dokl. Akad. Nauk. SSSR 132 (1960) 1307.
34) G.E. Nash and M.E. Glicksman, Acta Metall. 22 (1974) 1283.
35) J.S. Langer, Physicochemical Hydrodynamics 1 (1980) 41.
36) M.A. Chopra, Ph.D. Thesis, Rensselaer Polytechnic Inst. (1983).
37) A. Karma and J.S. Langer, Phys. Rev. A (to be published).
38) E. Ben-Jacob, N. Goldenfeld, J.S. Langer and G. Schön, Phys. Rev. 29A (1984) 330.
39) "String"-models in which V_n depends only on κ and $\partial^2\kappa/\partial s^2$ have been studied recently by R. Brower, D. Kessler, J. Koplik and H. Levine, Phys. Rev. Lett. 51 (1983) 1111.